CROATICA CHEMICA ACTA CCACAA **62** (4) 623—644 (1989)

YU ISSN 0011-1643
CCA-1893 UDC 541
Conference Paper

Semiempirical Study of Intramolecular Hydrogen Bond in Naphthazarin

Z. B. Maksić[a,b], *M. Eckert-Maksić*[a], *and D. Kovaček*[a]

[a]*Ruđer Bošković Institute, Bijenička c. 54, 41001 Zagreb, Croatia, Yugoslavia*
[b]*Faculty of Natural Sciences and Mathematics, The University of Zagreb, Marulićev trg 19, 41000 Zagreb, Croatia, Yugoslavia*

Received September 18, 1989

It is found that MINDO/3, MNDO and AM1 give a reasonable description of intramolecular hydrogen bonds in malonaldehyde, acetylacetone and naphtazarin tautomers as evidenced by comparison with the available ab initio results and reliable experimental findings. MINDO/3 and MNDO procedures offer information at a qualitative level, whilst AM1 yields semiquantitative results after some empirical adjustements.

The main result of this study is a strong indication that all studied systems possess asymmetric H-bond(s) at least in the gas phase. The most stable tautomer of naphthazarin has 1,4-quinoid structure. It is found that single proton (two step) tunnelling is energetically much more favourable than concerted (simultaneous) transfer of both protons. Tunnelling barrier heights, of internal H-bonds are thoroughly discussed and interpreted in terms of the micro- and gross-energy partitioning method. Variation in structural parameters and changes in atomic charges are elaborated. It is established that keto- and hydroxy-oxygens have substantially different electron densities, which necessarily lead to appreciable differences in their 1s ESCA shifts.

INTRODUCTION

A large number of molecules belonging to the general class of β-diketones and to the corresponding enol tautomers have attracted considerable interest in the last decades due to their extensive use as chelating ligands, their possible role in the process of vision, energy storage at the molecular level etc. The question of symmetry and structure of the intramolecular hydrogen bond is an interesting problem per se. It is not surprising, therefore, that β-diketones have been a subject matter of numerous experimental and theoretical studies. The latter employed a variety of methods ranging from simple semiempirical procedures to sophisticated extended basis set ab initio calculations. In spite of large research efforts, however, results pertaining O . . . H—O fragments of intramolecularly bonded protons are frequently contradictory- for several reasons. Some of the applied experimental techniques operate on too large time scales whereas the studied systems seem to undergo fast topomerization. Others based on scattering suffer from a drawbeck caused by the fact that hydrogen atom is a poor scatterer. Different answers provided by theory are a consequence of the use of inadequate basis sets and/or semiempirical schemes. This general pattern holds also for naphthazarin (Figure 1) studied in this paper. The reason why our attention was focused on this compound is two-fold: (a) it has an assembly of functional groups which occur in chemically important antitumor antibiotics[1] and (b) the minimum basis set STO-3G calculations on naphthazarin tautomers are available[2]. Hence, we can check our semiempirical MNDO and AM1 results against more rigorous *ab initio* predictions. This is of importance because experimental data are not unequicoval and the semiempirical methods have to be tested regarding their credibility.

Empirical findings concerning naphthazarin structure are controversial. We shall discuss its features in solution first. Yosien et al.[3] proposed the

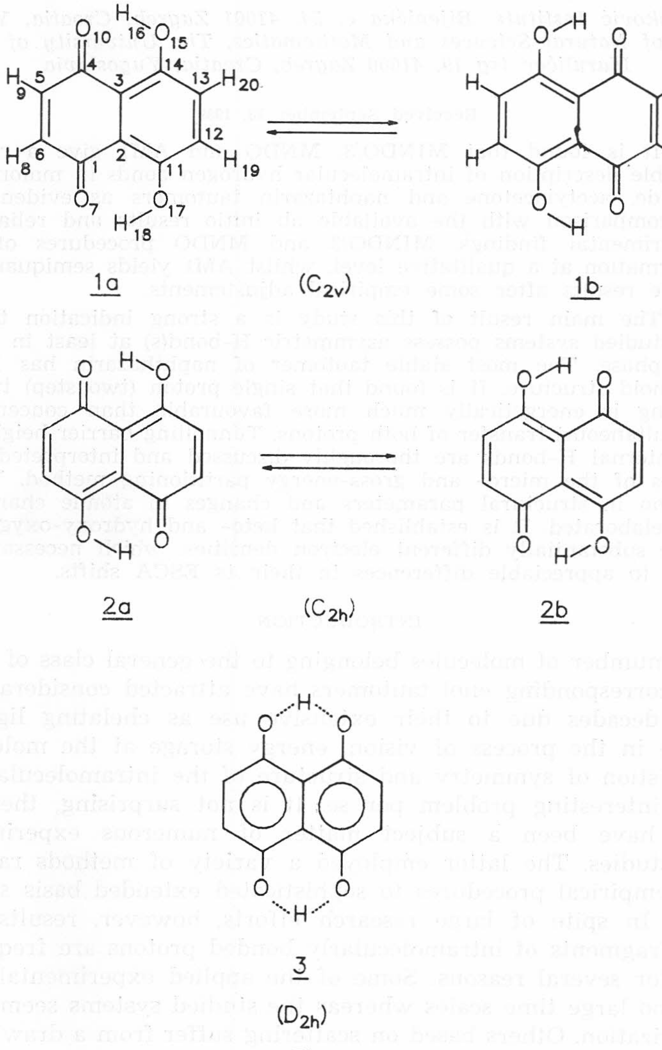

Figure 1.

structure *3* (D_{2h}) with symmetrical H-bonds and enhanced bond delocalization. On the contrary, Hadži and Sheppard[4] have shown that intramolecular H-bonds are definitely not symmetric, instead, protons move in asymmetrical double minimum potential. The latter corresponds to the two equivalent 1,4-quinoid geometries *1* (C_{2v}). Incidentally, Merian proposed the 1,5-quinoid geometry *2* (C_{2h}) as the most stable one[5], which completes all structures presented in Figure 1. Bratan and Strohbush[6] measured IR and NMR spectra of naphthazarin in certain solutions. They concluded that the compound assumes the two centrosymmetric structures *2a* and *2b* (C_{2h}) which are interconverted by the tunnelling of the two protons at such a high rate that only their average, *i. e.* effective, symmetry is observed in IR and NMR measurements. On the other hand, NMR experiments by others[8] indicate that the two equivalent structures with hydroxyl groups attached to the same ring are in a rapid equilibrium. An indirect argument has been made that this structure (C_{2v}) is substantially more stable than 1,5-quinone geometry (C_{2h})[9].

Solid state studies are usually compatible with asymmetric arrangement of H-bonds. The X-ray structural investigation of Cradwick and Hall[7] have led to the unusual conclusion that heavy atoms assume symmetrical (D_{2h}) arrangement in contrast to the phenolic hydrogens which are asymmetrical. The results were interpreted in terms of the resonance of peculiar zwitterionic canonical structures of the 1,5-quinone type. The ^{13}C NMR spectra obtained by using the »magic angle« spinning technique strongly suggest that the structure of solid naphthazarin is dynamically disordered involving a tautomeric equilibrium which is very fast at room temperature[10]. Finally, de la Vega *et al.*[2] found by STO-3G calculations that structure *1* is the absolute minimum on the potential energy surface, *2* is a saddle point whilst *3* is the absolute maximum. Structures *2* and *3* are 25.0 and 28.0 (kcal mol^{-1}) above the equilibrium arrangement of atoms *1*, respectively.

In view of the wide variety of suggestions concerning the structure of naphthazarin, we felt that additional theoretical studies were worthwhile. Since the system is quite sizeable, semiempirical treatments are in place. It is generally accepted by now that the MINDO/3 method is completely inappropriate for studying hydrogen bonding[11,12]. We shall comment on that later on. There is a widespread opinion that the same holds for MNDO method. While this is true for intermolecular hydrogen bonds, we were pleasantly surprised with the performance of both approaches in revealing the basic features of intramolecular H-bonding. MNDO and MINDO/3 schemes gave a correct ordering in stability of vitamin C tautomers, predicted the site of protolitic hydrogen in accordance with experience, provided qualitatively good structural parameters and offered an essentially correct interpretation of intramolecular H-bonds[14]. Similar results were obtained for a number of 3-substituted tetronic and 3-acetyl tetramic acids[15]. Hence, the use of the MNDO approach in the present study seems to be justified. The refined version AM1 should perform even better. Recent results on nitro — enamines show that the AM1 method is comparable to STO-3G and 3—21G treatments of intramolecular H-bonds. Anticipating the forthcoming results on naphthazarin, we can say that the MNDO, MINDO/3 and AM1 methods support the findings of de la Vega *et. al.*[2]

RESULTS AND DISCUSSION

MNDO[17] and AM1[18] methods were used in their original versions. Full optimization of all independent structural parameters is performed.

Both methods were applied first to enol forms of malonaldehyde (MA) *4* and acetyl — acetone (ACAC) *5*. They represent prototypes of internally H-bonded systems (Figure 2). Since they are relatively small, a number of theoretical results exsits in the literature. The early CNDO/2 calculation of Schuster[19] suggested asymmetrical internal H- bond in MA. The energy separating two C_s minima was extremely small (0.5 kcal mol^{-1}). However, the geometry of O . . . H—O fragment was only optimized. INDO calculations predicted, however, the C_{2v} structure as the most stable one.[20] The same result was obtained by the ab initio method, but with partial geometry optimization[21] of MA. On the other hand, the complete geometry optimized structure with STO-3G basis set[22] indicates that C_s form is more stable by 6.6 kcal mol^{-1}. This example provides a nice illustration of the importance of geometry optimization and that introduction of arbitrary constraints and standard bond distances causes undesirable bias. Extended basis set SCF study of MA[23] suggest that the H- bond potential is of the double- well type with a barrier height of 11.5 kcal mol^{-1}. This barrier drops to 10 kcal mol^{-1} if electron correlation is taken into account which is of course more pronounced in the C_{2v} structure[24]. Both calculations, SCF and SCF + CI, are somewhat invalidated by the fact that the geometry optimization was only partial. Similar results were obtained by slightly better than the DZ basis set[36a] at SCF and SCF + all single and double excitations CI levels *(vide infra)*.

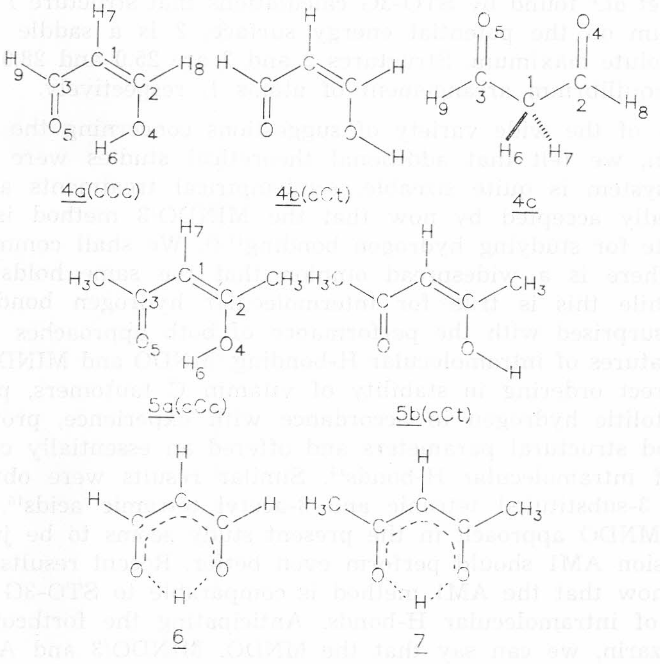

4a(cCc) 4b(cCt) 4c

5a(cCc) 5b(cCt)

6 7

Figure 2.

Finally, full optimization with the double zeta 4-31G basis set shows that the ground state of MA has C_s structure[25]. SCF calculation with the same basis set (4-31G) revealed a double minimum profile along the reaction coordinate[26] with a barrier between the two equivalent C_s structures of 11.6 kcal mol^{-1}. It was found that proton oscillates between the two wells with a frequency of $0.7 \cdot 10^{11}$ s^{-1}. Calculations employing a large basis set (6-31G**) and involving electron correlation at the MP2 level[36b] will be considered somewhat later.

The most reliable experimental evidence is also in favour of the C_s structure of MA and ACAC. However, the early electron diffraction (ED) measurements on ACAC were interpreted by a linear and symmetric intramolecular H-bond[27]. The same conclusion was drawn by the ED study of hexafluoro — ACAC[28]. In contrast, Iijima *et al.*[29a] found in their ED investigation of ACAC that the molecule is asymmetric. Remarkably, the »hydrogen bonded« proton is found to be significantly out of plane of heavy atoms. Bond localization and asymmetric H-bond was found in the X-ray crystal structure study of ACAC[29b]. There is also a rich spectroscopic evidence indicating that enolic hydrogen bond in MA and ACAC is asymmetric: ^{13}C and ^{2}H spin lattice relaxation time measurements[30], estimates of deuteron quadrupole coupling constants (DQCC)[31] MW spectra[32] and ESCA chemical shifts[33]. The latter technique is very reliable because it is extremely fast (10^{-16} s) thus yielding an »instantaneous« snapshot of the molecule. In any case, its time scale is sufficient to differentiate between the terminal oxygens in spite of the extremely rapid $O \cdots H—O \Longleftrightarrow O—H \cdots O$ topomerization. In this connection it should be mentioned that our semiempirical SCC—AMEP model[34] proved useful in assigning O(1s) ESCA shifts in MA, ACAC and related compounds which established the existence of asymmetric $O \cdots H—O$ fragment[35].

Summing up reliable experimental and theoretical results, one concludes that it is beyond reasonable doubt that the intramolecular H-bond in MA, ACAC and related systems is asymmetric in nature.

Let's compare the present semiempirical and earlier *ab initio* results in more detail (Table I). Perusal of the data shows that the MNDO and AM1

TABLE I

Comparison of structural parameters in MA and ACAC obtained by the MNDO and AM1 methods with the available ab initio *and experimental results (in Å and degrees)*

Molecule	Bond(s)	4-31G	MNDO	AM1	Ab initio or exptl.
4a	$C_1{=}C_2$	1.340^a	1.362	1.352	1.33^b; 1.347^c; 1.348^d; 1.361^f; 1.362^h
	C_1—C_3	1.441	1.472	1.452	1.48; 1.456; 1.454; 1.455; 1.439
	C_2—O_4	1.336	1.342	1.353	1.36; 1.336; 1.320; 1.346; 1.328
	$C_3{=}O_5$	1.231	1.227	1.241	1.23; 1.240; 1.234; 1.239; 1.248
	O_4—H_6	0.981	0.949	0.976	1.00; 0.960; 0.969; 0.959; 0.994
	C_1—H_7	1.073	1.095	1.100	1.08; 1.10; 1.091; 1.069; 1.077
	C_2—H_8	1.074	1.103	1.107	1.09; 1.10; 1.089; 1.071; 1.083
	C_3—H_9	1.087	1.111	1.113	1.10; 1.10; 1.094; 1.082; 1.098
	$O_4 \ldots O_5$	2.659	3.172	2.845	2.561; 2.63; 2.553; 2.625; 2.589
	C_2—O_4—H_6	112.9°	115.9°	110.8°	104°; 110.9°; 106.4°; 112.5°; 105.4°
	C_1—C_2—C_4	125.7°	129.6°	127.0°	125°; 124.4°; 124.5°; 129.9°; —
	C_3—C_1—C_2	121.2°	131.1°	124.9°	119°; 128.8°; 119.4°; 121.4°; —
	C_1—C_3—C_5	123.6°	125.8°	123.9°	122°; 123.2°; 123.0°; 123.3°; 123.5°

Table I (contd.)

4b	$C_1=C_2$	1.325[a]	1.359	1.348	
	C_1—C_3	1.457	1.478	1.459	
	C_2—O_4	1.352	1.349	1.366	
	$C_3=O_5$	1.214	1.223	1.233	
	C_4—C_6	0.963	0.948	0.968	
	O_1—H_7	1.076	1.094	1.101	
	C_2—H_8	1.078	1.101	1.104	
	C_3—H_9	1.091	1.112	1.116	
	$O_4 \ldots O_5$	2.902	3.011	2.785	
4c	$C_1=C_2$		1.524	1.497	
	C_1—C_3		1.524	1.497	
	C_2—O_4		1.218	1.227	
	$C_3=O_5$		1.218	1.227	
	C_1—H_7		1.116	1.125	
	C_2—H_8		1.112	1.116	
	C_3—H_9		1.112	1.116	
	$O_4 \ldots O_5$		2.964	2.751	
	C_1—C_2—O_4		126.8°	125.6°	
	C_3—C_1—C_2		112.0°	113.0°	
	C_1—C_3—O_5		126.8°	125.6°	
5a	$C_1=C_2$		1.372	1.357	1.382[e]; 1.338[g]
	C_1—C_3		1.481	1.454	1.430; 1.412
	C_2—O_4		1.347	1.360	1.319; 1.331
	$C_3=C_5$		1.232	1.245	1.243; 1.238
	O_4—H_6		0.947	0.975	1.049; 1.03
	C_1—H_7		1.095	1.100	1.099; —
	C_2—C_m		1.522	1.489	1.525; 1.478 (1.554)
	C_m—H		1.108	1.118	1.105; —
	$O_4 \ldots O_5$		3.066	2.821	2.512; 2.535
	C_2—O_4—H_6		116.2°	110.4°	81.0°; 96.0°
	C_1—C_2—O_4		126.9°	125.9°	121.0;° 122.8°
	C_3—C_1—C_2		131.0°	125.2°	119.7°; 122.2°
	C_1—C_3—O_5		122.9°	123.1°	123.0°; 120.5°
5b	$C_1=C_2$		1.367	1.354	
	C_1—C_3		1.487	1.461	
	C_2—O_4		1.354	1.370	
	$C_3=C_5$		1.229	1.238	
	O_4—H_6		0.948	0.969	
	C_1—H_7		1.095	1.101	
	C_2—C_m		1.516	1.487	
	C_m—H		1.109	1.118	
	$O_4 \ldots O_5$		2.869	2.718	
	C_2—O_4—H_6		116.1°	108.6°	
	C_1—C_2—O_4		116.9°	119.3°	
	C_3—C_1—C_2		136.6°	125.8°	
	C_1—C_3—O_5		129.1°	124.3°	
6	C_1—C_2		1.420	1.404	1.40[b]; 1.390[c]; 1.401[f]
	C_2—O_4		1.286	1.296	1.29; 1.283; 1.291
	$O_4 \ldots H_6$		1.223	1.237	1.168; 1.182; 1.191
	C_2—H_8		1.100	1.106	1.100; 1.100; 1.075
	C_1—H_7		1.083	1.092	1.07; 1.100; 1.066
	$O_4 \ldots O_5$		2.333	2.598	2.29; 2.29; 2.308
	C_2—O_4—H_6		109.5°	108.9°	102.4°; 105.7°; 109.5°
	C_1—C_2—O_4		119.2°	120.8°	121.0°; 121.5°; 120.8°
	C_3—C_1—C_2		117.4°	116.7°	; 114.8°; 115.6°

---

[a] Ref. 25; [b] Ref. 22; [c] Partial DZ geometry optimization[23]; [d] MW data[32], [e] ED data[29(a)]; [f] Slightly better than DZ basis set[36a]; [g] X-ray data of Ref. 29(b); [h] 6-31G** MP2 calculation to Ref. 36(b).

methods offer a good description of the bond distances and bond angles in malonaldehyde (MA) *4a*. They are in particularly good accordance with a »better than DZ« basis set of Schaefer *et al.*[36] Larger discrepancy is found in estimates of the $O_4 \cdots O_5$ nonbonding contact, but *ab initio* at the SCF level does not generally reproduce the experiment either. The latter lies in an isotopic range of 2.553—2.576 Å[32] and only the electron correlation by the MP2 formalism brings theory close to the upper bound of this range[36b]. The MNDO exceeds the bridgehead distance of the internal hydrogen bond by 0.60—0.62 Å whereas AM1 diminishes this discrepancy by 50% yielding a value in the range of 0.27—0.29 Å. Schaefer's *ab initio* is off by 0.11—0.13 Å offering a further improvement. 6-31G** MP2 approach yields 2.589 Å for $O \cdots O$ contact indicating that the electron correlation should be explicitly taken into account. We shall use these values for empirical adjustments of the MNDO and AM1 results in more complex molecules. The symmetric structure *6* is also well reproduced. Comparison of MNDO and AM1 results for geometry of ACAC exhibits large discrepancies with both ED and X-ray estimates (Table I). However, these two techniques give very different data themselves. A common feature is the pronounced localization obtained by the theoretical and experimental methods applied. Another striking feature is that they all predict a shortening of $O_4 \cdots O_5$ contact relative to the parent MA compound. Gas-phase ED found a strong out-of-plane displacement of the H_6 atom. It should be mentioned that in both enol forms of MA and ACAC the hydrogen bonded proton is found to lie in the plane of heavy atoms by the semiempirical theory. Extended basis set *ab initio* calculations are probably necessary to settle the problem. It follows that the MNDO and AM1 methods give a reasonable description of gross features like the shape and size of β-diketones.

Energetic properties deserve a close scrutiny, too. The estimated heats of formation are given in Table II. One observes that the asymmetric intra-

TABLE II

Bicentric energy terms, gross energy partitioning and heats of formation, as estimated by MNDO and AM1 methods (in eV and kcal mol^{-1}, respectively)

Molecule	Atomic pairs	MNDO	AM1
4a	$C_1{=}C_2$	—23.3	—22.4
	C_1—C_3	—17.0	—16.5
	C_2—O_4	—18.4	—16.9
	$C_3{=}O_5$	—26.9	—25.0
	O_4—H_6	—14.1	—12.7
	C_1—C_7	—13.0	—12.9
	C_2—H_8	—12.7	—12.2
	C_3—H_9	—12.5	—12.0
	$O_5 \ldots H_6$	— 0.4	— 0.8
	$O_4 \ldots O_5$	0.3	0.3
4b	$C_1{=}C_2$	—23.4	—22.6
	C_1—C_3	—16.6	—16.0
	C_2—O_4	—17.9	—16.3
	$C_3{=}O_5$	—27.2	—25.5
	O_4—H_6	—14.1	—12.9
	C_1—H_7	—13.0	—12.8
	C_2—H_8	—12.8	—12.4
	C_3—H_9	—12.4	—12.0

Table II (contd.)

Molecule	Atomic pairs	MNDO	AM1
	$O_5 \ldots H_6$	— 0.2	— 0.2
	$O_4 \ldots O_5$	0.4	0.3
	$H_6 \ldots H_8$	0.2	0.2
4c	$C_1{=}C_2$	—14.8	—14.5
	C_1—C_3	—14.8	—14.5
	C_2—O_4	—27.5	—26.0
	$C_3{=}O_5$	—27.5	—26.0
	C_1—H_7	—12.3	—12.1
	C_2—H_8	—12.4	—12.0
	C_3—H_9	—12.4	—12.0
	$O_4 \ldots O_5$	0.3	0.3
6	C_1—C_2	—20.3	—19.6
	C_2—O_4	—22.7	—21.1
	$O_4 \ldots H_6$	— 6.9	— 6.6
	C_1—H_7	—13.4	—13.2
	C_2—H_8	—12.6	—12.1
	$O_4 \ldots O_5$	— 0.1	—0.18

molecular hydrogen bonded enol form *4a* of MA is the most stable species. The corresponding difference in energy is 39.0 and 22.1 (in kcal mol^{-1}) for MNDO and AM1 methods, respectively. This should be compared with *ab initio* results at the SCF level discussed earlier. STO-3G[22] and DZ basis sets[23] gave 10.3 and 11.5 kcal mol^{-1}, respectively. Schaefer *et al.*[36a] estimate 11.4 kcal mol^{-1}, as a barrier height, a value which drops to 8.0 kcal mol^{-1} if massive CI employed. Additional 6-31G** MP2 and MP4 calculations[36b] yield 3.6 and 4.3 kcal mol^{-1} respectively, being close to the experimental data[32] lying in

Gross energy partitioning and heats of formation

Molecule	Entities	MNDO	AM1	Δ (MNDO)	Δ (AM1)
4a	ΔH_f	—70.9	—71.0	0	0
	E_1^t	—951.9	—952.1	0	0
	E_2^t (b)	—137.8	—131.5	0	0
	E_2^t (nb)	5.3	3.8	0	0
4b	ΔH_f	—68.3	—61.7	2.6	9.3
	E_1^t	—952.3	—952.4	—	—0.3
	E_2^t (b)	—137.3	—130.1	—	1.0
	E_2^t (nb)	5.3	3.1	—	—0.3
4c	ΔH_f	—68.1	—67.0	2.8	4.0
	E_1^t	—955.4	—954.2	—	—2.1
	E_2^t (b)	—133.9	—129.2	—	2.3
	E_2^t (nb)	5.0	3.8	—	0
6	ΔH_f	—31.9	—48.9	39.0	22.1
	E_1^t	—951.4	—951.5	—	0.6
	E_2^t (b)	—138.4	—131.9	—	0.5
	E_2^t (nb)	7.1	4.6	—	0.8

the range 4.0—5.2 kcal mol^{-1}. One can conclude that MNDO and AM1 overestimate the instability of the transition structure, the latter method being substantially more realistic. They are both qualitatively correct, however. Similar results were obtained for the ACAC where MNDO and AM1 methods estimate proton tunnelling barrier as high as 35.2 and 20.8 (in kcal mol^{-1}), respectively. One observes a slight decrease by CH_3-substitution relative to the parent compound MA. The intramolecular H-bond strenght can be roughly estimated by the energy difference between *4a* and *4b*. AM1 yields 9.3 kcal mol^{-1} which can be favourably compared with the DZ result[25] of 13.3 kcal mol^{-1}. MNDO offers a too low value of ~3 kcal mol^{-1}. Schaefer *et al.*[36b] obtained for this difference values of 12.0, 12.4 and 11.8 kcal mol^{-1} for DZ+P, 6-31G** and 6-31+G** basis sets, respectively. Notice that they erroneously refer to *4b* (cCt) as a keto-form.

Finally, MNDO and AM1 methods indicate that the enol form of MA is more stable than β-diketone tautomer by 2.8 and 4.0 kcal mol^{-1}, respectively, in accordance with the empirical findings that the enol form usually predominates in this family of compounds.

It would be very useful to get an idea about the possible reasons for the energetic variation presented above. For this purpose, we shall make use of the energy partitioning technique[37–39] which gives a useful insight into energy changes caused by intramolecular transformations. Generally, the total molecular energy can be expressed as a sum of one-center and two-center terms at the semiempirical level. However, it is convenient to group these matrix elements of the hamiltonian into three gross contributions: single center terms (E_1^t), two-center bonding interactions of the directly bonded atoms (E_2^t (b)) and the rest which corresponds to a sum of nonbonding two-center-interactions (E_2^t (nb)). The single center E_1^t term is by far the largest contribution, which is compatible with the idea of a modified atom in a molecule. On the other hand, the E_2^t (nb) term is the smallest indicating that nonbonding repulsions are not so important as some people think. They are by no means negligible, however. The AM1 results of the gross-energy partitioning for systems *4a*—*4c* and *6* are given in Table II. They show, for example, that the ground state of MA *4a* has two-center bonding energy E_2^t (b) by —1.0 eV lower than *4b*. A closer examination reveals that as much as —0.8 eV is a consequence of $O_5 \cdots H_6$ interaction, which is not present in *4b*. Further, *4b* has slightly lower NB-interactions and somewhat lower one-center energies. A connection of the latter with formal atomic charges (Table III) is interesting. Athough there are exceptions, a simple rule of thumb can be deduced stating that the higher electron density on atom roughly leads to lower single-center energy. In other words, nuclear-electron attraction outweighs electron repulsion within the atomic domain.

Keto-enol tautomerism in the picture of energy partitioning gives, the following main results. Bonding part E_2^t (b) is substantially lower (2.3 eV) in *4a* relative to *4c*. The main contributions come from the intramolecular $O_5 \cdots H_6$ bonding ~ —0.8 eV. Interestingly, rearrangement of the skeleton O_4—C_2—C_1—C_3—O_5 leading from *4a* to *4c* does not contribute almost anything to a change in the E_2^t (b) term. Finally, C_2—H_8 and C_3—H_9 bonds are more stable in *4a* by 0.2 eV than their counterparts in *4c*. In contrast the E_1^t

energy is by —2.1 eV lower in diketo-form *4c*. The largest single-center stabilization by transfer of the H_6 atom to the central C_1 atom is exhibited by O_4 oxygen (—1.2 eV), presumably due to rehybridization. Removal of hydrogen enables accommodation of its lone pairs in hybrids with high s-characters. The one-center energy of the H_6 atoms is also appreciably lower (—0.8 eV) in *4c* simply because its electron density is much higher (by —0.13 eV) than in *4a*, where the H-bonded proton possesses a small portion of electron charge. It is worth mentioning that the O_5 atom undergoes one-center destabilization (by 0.7 eV) because it loses in *4c* 0.1 $|e|$ of electrons. In contrast, C_3 and H_8 atoms gain in atomic stabilization by —0.5 eV each, because their electron density increases in *4c*.

Analysis of energy terms in symmetric form *6* is instructive. Two-center energy E_2^t (b) is lower than in the parent molecule *4a* (—0.5 eV) which is in accordance with the delocalized nature of the transition structure. This conclusion holds for each bond with one notable exception. The localized bridge O · · · H—O in *4a* is more stable than the delocalized symmetric arrangement O · · · H · · · O in *6* by —0.2 eV. Hence, the usual and superficial argument that the symmetric H-bond is more stable than the asymmetric one because of its intrinsic »aromaticity« is wrong. Analysis of one-center energies does not change this conjecture because they are slightly lower in *4a* for O_4, O_5 and H_6 atoms. The asymmetric H-bond in *4a* is more stable because it has lower one-center total energy (—0.6 eV) and smaller nonbonding interactions E_2^t (nb). A decisive net effect in the former is substantially lower single-center energy of atom C_2 in *4a* than in *6*, which is a consequence of a considerable decrease in electron density in the latter. Nonbonding two-center terms are relatively small but persistent. They are significant even between relatively distant atoms because of the long range Coulomb interaction particulary if formal atomic charges are sizeable. For instance, the nonbonding interaction between hydrogen atoms H_6 · · · H_7 is 0.22 eV in *6* whereas repulsion between C_2 · · · H_7 in the same structure is 0.69 eV. The corresponding values for *4a* system are 0.15 eV and 0.30 eV (if C_3 atom is in question, a value for C_3 · · · H_7 repulsion is 0.52 eV). Further, O_4 · · · O_5 repulsion are 0.32 eV and 0.66 eV in *4a* and *6*, respectively. Therefore, it is difficult to detect a dominant nonbonding effect because they have a pronounced variability. Important role of Coulomb repulsions here and the relevance of one-center energies underlines the fact that reliable estimates of atomic charge densities are crucial in semiempirical theories. To conclude the analysis of MA systems, we can say that *4a* is more stable than transition structure *6* because a decreased E_1^t single-center energy and diminished nonbonded repulsions in the ground state outweigh more favourable E_2^t (b) in the latter symmetric arrangement of bonds.

The calculated atomic charges by MNDO and AM1 for configurations of MA are reviewed in Table III. It should be stressed that effective charges of atoms in molecules are a very important ingredient of the MAM (modified atoms in molecules) model. A number of molecular properties can be described by the concept of atomic charge[40-42]. In our opinion, it is a pseudo-observable par excellence just like hybridization.

TABLE III

Formal atomic charges in MA systems, as calculated by MNDO and AM1 methods (in |e|).

	4a		*4b*		4c		*6*	
Atoms	MNDO	AM1	MNDO	AM1	MNDO	AM1	MNDO	AM1
C_1	—0.325	—0.412	—0.247	—0.330	—0.112	—0.303	—0.457	—0.507
C_2	0.200	0.109	0.152	0.054	0.255	0.183	0.327	0.229
C_3	0.316	0.231	0.306	0.221	02.55	0.183	0.327	0.229
O_4	—0.248	—0.254	—0.229	—0.221	—0.256	—0.244	—0.372	—0.370
O_5	—0.341	—0.345	—0.298	—0.285	—0.256	—0.224	—0.372	—0.370
H_6	0.222	0.260	0.197	0.216	0.042	0.128	0.320	0.353
H_7	0.071	0.150	0.062	0.140	0.042	0.128	0.089	0.157
H_8	0.087	0.164	0.053	0.124	0.015	0.084	0.069	0.139
H_9	0.017	0.010	0.005	0.080	0.015	0.084	0.069	0.139

Survey of the results shows that changes in atomic densities induced by O · · · H—O proton tunnelling or rotation of O—H bond (around the C_2—O_4 »rigid« one) are compatible with a simple electrostatic picture. For instance, if *4a* atomic charges are used as a gauge then one can infer that a decrease in electron densities of O_4 and O_5 atoms in *4b* is probably a consequence of a tendency of diminishing their Coulomb repulsions, because they are no longer screened by a »common« proton. Further, effective (positive) charges of hydrogens H_6 and H_8 are diminished in *4b* because their distance is smaller than in *4a*. However this picture is plausible, it is a oversimplification. Hence, some caution should be exersized because a change in atomic density affects one-center energies the most. To be more specific, an increase in electron density of H_6 and H_8 atoms in *4b* lowers their single-center AM1 energies by —0.28 eV and —0.24 eV, respectively, whereas their nonbonded repulsion is increased by only 0.12 eV. Apparently, the one-center energy term is more decisive. It follows that a final charge distribution is a subtle interplay of a large number of one-center and two-center bonding and nonbonding terms.

For our purpose it is important to note that electron densities on oxygen O_4 and O_5 atoms are different in *4a* because they lead to different ESCA chemical shifts. Higher electron density at O_5 means that 1s(O_5) electron is more tightly bound in accordance with the experiment[33] and earlier semiempirical calculations[35]. This is highly significant because it provides evidence that the H-bond is truly asymmetrical. A symmetric bond would yield a single main peak. Our SCC-AMEP (Self-consistent charge-atomic monopole electrostatic potential) model has shown that keto- and enol-form can be clearly distinguished in the ESCA spectrum[35]. It would be interesting to find a corresponding correlation with AM1 charges.

Relative stabilities of naphthazarin tautomers *1a*, *2b*, *3*, and *8*—*15* (Fig. 3) in some characteristic conformations as obtained by the MINDO/3, MNDO and AM1 methods are given in Table IV. Results of these three approaches are in qualitative mutual agreement. According to the semiempirical theory, the most stable tautomer has two O—H groups attached to the same benzene nucleus (1,4 structure). Consequently, both H-bonds are asymmetric leading to the C_{2v} symmetry of *1*. This is in harmony with some careful experimental

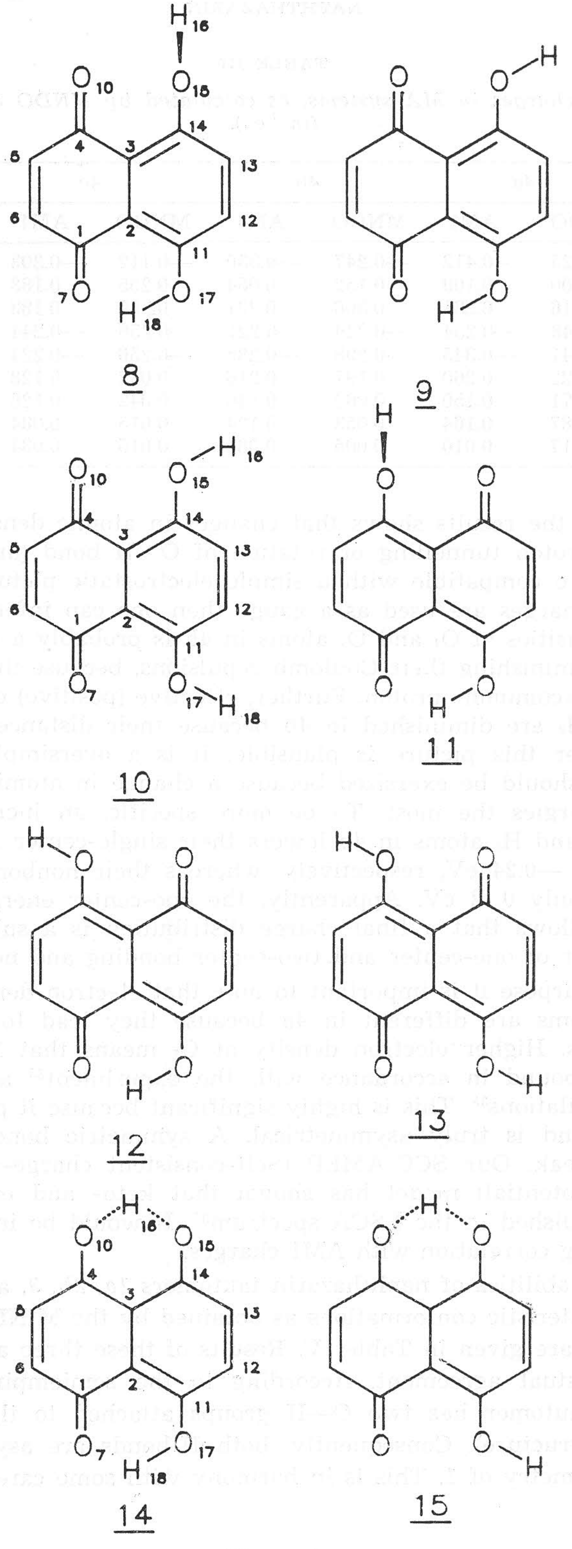

Figure 3.

TABLE IV

The calculated MINDO/3, MNDO and AM1 heats of formation of naphthazarin tautomers and for some of their conformations. Relative stabilities are denoted by Δ *(in kcal mol*$^{-1}$*).*

Compound	MINDO/3	MNDO	AM1	Δ (MINDO/3)	Δ (MNDO)	Δ (AM1)
1a	—133.8	—111.4	—105.8	0	0	0
2b	—127.8	—103.3	—97.1	6.0	8.1	8.7
3	—85.0	—37.6	—56.4	48.8	73.8	49.4
8	—130.1	—109.9	—99.5	3.7	1.5	6.3
9	—132.2	—111.0	—100.5	1.6	0.4	5.3
10	—130.5	—110.3	—95.1	3.3	1.1	10.7
11	—122.4	—100.0	—87.4	11.4	11.4	18.4
12	—125.3	—101.5	—88.2	8.5	9.9	17.6
13	—122.9	—99.8	—82.5	10.9	11.6	23.3
14	—111.0	—76.0	—81.1	22.8	35.4	24.7
15	—109.3	—74.6	—74.9	24.5	36.8	30.9

studies[4,9,10] as discussed earlier and with the minimal basis set *ab initio* results[2]. The 1,5-quinoid structure *2* (C_{2h}) is ~ 6—9 kcal mol^{-1} less stable, whilst the two symmetric internal H-bonds in *3* (D_{2h}) represent a transition structure which is ~ 50—74 kcal mol^{-1} above the ground state. The corresponding *ab initio* STO-3G numbers are 25 and 28 kcal mol^{-1}, respectively. Hence, it seems that semiempirical methods overestimate the barrier height for simultaneous proton tunnelling and underestimate the instability of tautomer *2*. Barrier for asynchronous proton tunnelling is substantially (by $50^{0}/_{0}$) lower according to the semiempirical theory. It should be pointed out that in two-step proton transfer the second proton faces a barrier height which is even smaller than ~ 25 kcal mol^{-1} (on the AM1 energy scale) obtained as a difference *E(14)—E(1a)*. The point is that the tunnelling of the first proton produces tautomer *2b* which is by 9 kcal mol^{-1} less stable than 1a. Consequently, the barrier height for the second proton transfer producing back tautomer *1b* is 16 kcal mol^{-1} according to the AM1 results. Rotation barriers of the O—H bond around the »rigid« C—O bond emanating from the benzene ring are relatively low; ~ 2—6 kcal mol^{-1} for tautomer *1* and ~ 11—18 kcal mol^{-1} for 1,5-quinoid form *2*. The higher numbers correspond to the AM1 results which are expected to be more reliable. A point of interest is of course the question of strength of the H-bond (s). An approximate criterion is given by comparison of the stabilities of structures *9* and *10* relative to *1a*. Analogously, a difference in ΔH_f values between *12, 13* and *2b* will give a rough estimate of single and double H-bonds in tautomer *2*. It appears that the MINDO/3 and MNDO methods yield substantially lower O · · · H bond energies than AM1. Since the latter scheme gave intramolecular hydrogen bond strengths which were comparable to *ab initio* estimates in small systems like MA, we infer that the AM1 results are more accurate. Hence, the

TABLE V

Geometry of 1a, 2b *and* 3 *systems, as obtained by MNDO and AM1 methods and their comparison with STO-3G results*[2]
Bond distances and angles (Å and degrees)

	1a			*2b*			*3*		
Atomic pairs	MNDO	AM1	STO-3G	MNDO	AM1	STO-3G	MNDO	AM1	STO-3G
C_3—C_4	1.501	1.472	1.500	1.397	1.379	1.439	1.436	1.417	1.398
C_3—C_{14}	1.419	1.399	1.403	1.501	1.465	1.462	1.436	1.417	1.398
C_4—O_{10}	1.232	1.243	1.239	1.346	1.357	1.378	1.288	1.300	1.298
C_{14}—O_{15}	1.350	1.366	1.378	1.234	1.247	1.239	1.288	1.300	1.298
C_4—C_5	1.495	1.475	1.508	1.481	1.456	1.447	1.480	1.459	1.492
C_{13}—C_{14}	1.450	1.426	1.413	1.491	1.471	1.485	1.480	1.459	1.492
$C_5=C_6$	1.343	1.335	1.320	1.348	1.342	1.347	1.365	1.354	1.334
$C_{12}=C_{13}$	1.371	1.368	1.374	1.349	1.342	1.347	1.365	1.354	1.334
C_1—C_6	1.495	1.475	1.508	1.487	1.470	1.485	1.480	1.459	1.492
C_{11}—C_{12}	1.449	1.426	1.413	1.475	1.456	1.447	1.480	1.459	1.492
C_2—C_{11}	1.415	1.398	1.403	1.397	1.379	1.439	1.436	1.417	1.398
C_1—C_2	1.498	1.472	1.500	1.495	1.466	1.462	1.436	1.417	1.398
C_2—C_3	1.464	1.429	1.407	1.486	1.453	1.407	1.435	1.419	1.430
$C_1=O_7$	1.233	1.243	1.239	1.233	1.247	1.239	1.288	1.300	1.298
O_{15}—H_{16}	0.945	0.971	1.995	2.185	1.949	1.574	1.229	1.249	1.204
O_{17}—H_{18}	0.945	0.971	1.995	0.946	0.974	0.995	1.229	1.249	1.204
C_{11}—O_{17}	1.350	1.366	1.378	1.346	1.357	1.378	1.288	1.300	1.298
$O_{10}\cdot\cdot H_{16}$	2.180	1.950	1.577	0.947	0.974	0.995	1.229	1.249	1.204
$O_7\cdot\cdot H_{18}$	2.180	1.950	1.577	2.179	1.947	1.574	1.229	1.249	1.204
$O_{10}\cdot\cdot O_{15}$	2.851	2.731	2.505	2.853	2.727	2.506	2.357	2.393	2.394
$O_7\cdot\cdot O_{17}$	2.851	2.731	2.505	2.853	2.726	2.506	2.357	2.393	2.394

TABLE V (contd.)

Bond distances and a ngles (Å and degrees)

	1a			*2b*			*3*		
Atomic pairs	MNDO	AM1	STO-3G	MNDO	AM1	STO-3G	MNDO	AM1	STO-3G
C_3—C_4—C_5	118.6^0	117.8^0	117.6^0	122.2^0	121.6^0	120.1^0	118.2^0	118.3^0	115.9^0
C_3—C_{14}—C_{13}	122.0^0	121.0^0	118.5^0	118.4^0	117.7^0	116.1^0	118.2^0	118.3^0	115.9^0
C_3—C_4—O_{10}	123.0^0	122.9^0	120.4^0	127.9^0	126.9^0	119.7^0	118.1^0	119.6^0	121.1^0
C_3—C_{14}—O_{15}	127.4^0	126.5^0	120.5^0	123.0^0	122.5^0	121.2^0	118.1^0	119.6^0	121.1^0
C_4—O_{10}—H_{16}	15.5^0	102.8^0		117.7^0	111.5^0	104.4^0	109.0^0	107.7^0	100.2^0
C_4—C_3—C_{14}	122.9^0	120.7^0	119.1^0	122.3^0	118.9^0	119.2^0	118.8^0	118.7^0	117.8^0
C_2—C_3—C_4	119.2^0	120.2^0	120.4^0	118.6^0	119.6^0	119.6^0	120.6^0	120.6^0	121.1^0
C_2—C_3—C_{14}	117.9^0	119.1^0	120.5^0	118.9^0	119.2^0	121.2^0	120.6^0	120.6^0	121.1^0
C_4—C_5—C_6	122.2^0	122.0^0	122.1^0	120.8^0	120.4^0	120.2^0	121.2^0	121.1^0	122.0^0
C_5—C_6—C_1	122.2^0	122.2^0	122.1^0	121.1^0	121.6^0	121.7^0	121.2^0	121.1^0	122.0^0
C_6—C_1—C_2	118.6^0	117.8^0	117.6^0	118.4^0	117.7^0	116.1^0	118.2^0	118.3^0	118.3^0
C_1—C_2—C_3	119.3^0	120.0^0	120.4^0	118.9^0	119.2^0	121.2^0	120.6^0	120.6^0	121.1^0
C_3—C_2—C_{11}	117.9^0	119.0^0	120.5^0	118.6^0	119.6^0	119.6^0	120.6^0	120.6^0	121.1^0
C_{14}—O_{15}—H_{16}	117.7^0	111.4^0	100.5^0	108.0^0	102.7^0		109.0^0	107.7^0	100.2^0
C_{11}—O_{17}—H_{18}	117.7^0	111.3^0	100.5^0	117.7^0	111.5^0	104.4^0	109.0^0	107.7^0	100.2^0

Table V (contd.)

	14		*9*		*12*	
Atomic pairs	MNDO	AM1	MNDO	AM1	MNDO	AM1
C_3—C_4	1.446	1.424	1.510	1.478	1.393	1.385
C_3—C_{14}	1.446	1.424	1.418	1.401	1.505	1.463
C_4—O_{10}	1.287	1.299	1.227	1.236	1 352	1.362
C_{14}—O_{15}	1.287	1.299	1.355	1.372	1.229	1.244
C_4—C_5	1.378	1.462	1.498	1.479	1.473	1.449
C_{13}—C_{14}	1.459	1.444	1.435	1.415	1.497	1.471
$C_5=C_6$	1.350	1.341	1.342	1.335	1.350	1.342
C_{12}—C_{13}	1.367	1.359	1.380	1.374	1.348	1.342
C_1—C_6	1.504	1.481	1.494	1.475	1.492	1.477
C_{11}—C_{12}	1.476	1.443	1.439	1.422	1.479	1.462
C_2—C_{11}	1.402	1.385	1.420	1.403	1.397	1.374
C_1—C_2	1.498	1.468	1.505	1.474	1.495	1.475
C_2—C_3	1.454	1.429	1.448	1.419	1.485	1.452
$C_1=O_7$	1.231	1.244	1.231	1.243	1.235	1.244
O_{15}—H_{16}	1.216	1.237	0.949	0.970	3.539	1.913
O_{17}—O_{18}	0.946	0.972	0.945	0.971	0.946	0.972
C_{11}—O_7	1.351	1.104	1.353	1.367	1.344	1.362
$O_{10}\cdot\cdot H_{16}$	1.218	1.237	3.519	3.404	0.949	0.972
$O_7\cdot\cdot H_{18}$	2.280	2.014	2.180	1.965	2.186	3.501
$O_{10}\cdot\cdot O_{15}$	2.325	2.362	2.621	2.471	2.640	2.728
$O_7\cdot\cdot O_{17}$	2.950	2.802	2.855	2.751	2.851	2.558
C_3—C_4—C_5	119.7	119.2	117.7	116.5	122.1	122.7
C_3—C_{14}—C_{13}	119.7	118.4	121.4	121.2	117.4	117.3
C_3—C_4—O_{10}	119.3	120.5	123.8	123.0	119.7	109.6
C_3—C_{14}—O_{15}	119.3	120.5	119.0	117.5	123.9	123.1
C_4—O_{10}—H_{16}	95.8	108.6	93.7	94.9	113.6	110.2
C_4—C_3—C_{14}	115.8	116.4	121.0	119.2	121.5	123.4
C_2—C_3—C_4	122.1	121.8	120.0	121.5	119.5	118.1
C_2—C_3—C_{14}	122.1	121.8	119.0	119.4	118.9	118.6
C_4—C_5—C_6	120.0	120.1	122.3	122.3	120.6	120.5
C_5—C_6—C_1	123.0	123.0	122.1	122.5	121.5	121.4
C_6—C_1—C_2	118.4	117.3	118.6	117.6	118.1	117.1
C_1—C_2—C_3	119.4	118.6	119.3	119.5	118.2	120.2
C_3—C_2—C_{11}	117.9	117.9	118.2	118.8	119.0	121.3
C_{14}—O_{15}—H_{16}	111.7	108.6	113.2	108.0	92.6	100.2
C_{11}—O_{17}—H_{18}	116.4	110.1	117.4	111.0	117.9	110.2

single $O\cdots H$ bond energy in *1* is ~ 5 kcal mol^{-1} as obtained by a difference $\Delta H_f(9) - \Delta H_f(1)$. If the model is close to reality, then the energy difference between *10* and *1* should be twice as much, i. e. ~ 10 kcal mol^{-1} which is indeed the case (Table IV). Interestingly, the hydrogen bond strength in *2* is much higher (by a factor ~ 3). Another point of interest is that H-bonds in *2* do not follow the simple additivity rule since two H-bonds in *13* are only ~ 5 kcal mol^{-1} stronger than a single $O\cdots H$ bond in *12*, according to the adopted energetic gauge. Obviously, the trans-or anti-bridge position of O—H bond is not always a good criterion for the strength of the internally bonded hydrogen. Hence, these values have to be used with due caution. Nevertheless, taking into account the results for MA (Table II), we can say that $O\cdots H$—O hydrogen bond strength increases along the series *1a* < *4a* < *2b*. Energies per single $O\cdots H$—O hydrogen bond in systems *1a* and *2b* are considered in these inequalities of course.

MNDO and AM1 structural parameters of *1a*, *2b* and *3* are compared with the minimum basis set *ab initio* bond distances and angles in Table V. Generally speaking, there is a good qualitative agreement between semiempirical and *ab initio* SCF results. The largest discrepancy is found for $O_{10} \cdots O_{15}$ and $O_7 \cdots O_{17}$ contacts which are overestimated in semiempirical methods. However, if empirical adjustement is employed for the AM1 results, a reasonable estimate of O · · · O distance is obtained in *1a* and *2b* tautomers. They lie in the range 2.44—2.46 Å which can be favourably compared with the STO-3G result (~ 2.51 Å). Surprisingly, AM1 and STO-3G are virtually the same in *3* which is fortuitous (2.39 Å). Empirical correction of the AM1 results indicates an even shorter O · · · O contact. In any case, we can say that symmetric intramolecular H-bonding induces a closer approach of O · · · O oxygens relative to the asymmetric case. It is of some interest to compare the O · · · O distances with the result of a parallel study performed on 6-hydroxy-2-formylfulvene (6—H2—FF) and 9-hydroxyphenalenone (9—HPO)[1]. Empirically corrected O · · · O distances read (Å):

	1a	2b	9-HPO(C_s)	5a	4a	6-H-2-FF(C_s)
d (O . . . O)	2.46	2.46	2.48	2.55	2.58	2.59

The results form two groups. It appears that *1a*, *2b* and 9-HPO (C_s) has practically the same O · · · O contacts. In the second group this nonbonding distance increases along the series *5a*, *4a* and 6-H-2-FF (Cs) from 2.55 Å to 2.59 Å being distinctly longer, compared to the members of the first group. Comparison of hypothetical symmetric hydrogen bonds yields:

	6-H-2-FF(C_{2v})	9-HPO(C_{2v})	3	6
d (O . . . O)	2.08	2.11	2.12	2.23

It follows that an appreciably larger O · · · O distance can be found in the transition structure of MA (*6*). Complex intramolecularly H-bonded systems 6-H-2-FF (C_{2v}), 9-HPO (C_{2v}) and naphtazarin (*3*) have comparable and shorter bridgehead O · · · O distances for the symmetric case than MA (*6*).

To conclude the discussion of structural characteristics of systems *1a*, *2b* and *3*, one can say that the latter exhibits delocalization, whereas *1a* and *2b* possess highly localized bonds which are schematically shown by Kekule structures in Figure 1. Naturally, some fragments are less localized than the others. For, example, bonds $C_2{=}C_{11}$ and $C_3{=}C_{14}$ in *1a* are somewhat delocalized, whereas localization is highly pronounced in $C_5{=}C_6$ and $C_{12}{=}C_{13}$ bonds. The same holds for system *2b* but the localization is slightly increased in it. Although the semiempirical (and STO-3G) structural parameters are highly approximate, relative values are more accurate. Hence, we believe that changes accompanying synchronous and asynchronous proton tunnelling, rotation of O—H bond and differences between tautomers are well reproduced. Data presented in Table V speak for themselves.

Results of the energy partitioning analysis are given in Table VI. We defer a detailed discussion to one of the next papers in this series because of the space limitation. It should be mentioned, however, that two center bonding terms are compatible with variation in bond distances. Gross energy partitioning components usually exhibit similar features observed in analysis of the archetypic molecule MA (Table II). For instance, AM1 differences in E_1^t, E_2^t (b) and E_2^t (nb) terms between *3* and *1a* are 1.4 eV, —2.4 eV and 3.1 eV, respectively, which is qualitatively comparable with the corresponding changes in going from *4a* to the transition structure *6* (0.6, —0.5, 0.8) (in eV). Higher values in the former case are a consequence of the presence of two internal H-bonds in *1a*. Tunnelling of the single proton (*14*) has the following components in the transition structure: (0.8, —1.4, 1.7). It is of some interest to compare the present results with a study of 6-hydroxy-2-formylfulvene and 9-hydroxyphenalenone[1]. Difference in energy between 6-H-2-FF (C_{2v}) and

TABLE VI

Two center energy terms (eV), as calculated by MNDO and AM1 methods and AM1 gross energy partitioning (in eV)

Atomic pairs	*1a*		*2b*		*3*	
	MNDO	AM1	MNDO	AM1	MNDO	AM1
C_3—C_4	—16.3	—15.8	—21.9	—20.9	—19.3	—18.7
C_3—C_{14}	—20.7	—19.8	—16.5	—16.2	—19.3	—18.7
C_4—O_{10}	—26.6	—25.0	—18.4	—17.0	—22.4	—20.9
C_{14}—C_{15}	—18.1	—16.6	—26.4	—24.6	—22.4	—20.9
C_4—C_5	—15.8	—15.3	—16.5	—16.1	—16.5	—16.2
C_{13}—C_{14}	—18.1	—17.9	—16.0	—15.6	—16.5	—16.2
$C_5{=}C_6$	—23.7	—23.1	—23.4	—22.6	—23.1	—22.4
$C_{12}{=}C_{13}$	—21.8	—20.9	—23.4	—22.6	—23.1	—22.4
C_1—C_6	—15.8	—15.3	—16.0	—15.6	—16.5	—16.2
C_{11}—C_{12}	—18.1	—17.8	—16.6	—16.1	—16.5	—16.2
C_2—C_{11}	—20.7	—19.8	—21.9	—20.9	—19.3	—18.7
C_1—C_2	—16.3	—15.8	—16.6	—16.2	—19.3	—18.7
C_2—C_3	—18.0	—17.7	—16.6	—16.2	—17.2	—16.7
$C_1{=}O_7$	—26.6	—24.9	—26.4	—24.6	—22.4	—20.9
O_{15}—H_{16}	—14.1	—12.6	—0.4	—0.9	—6.8	—6.5
O_{17}—H_{18}	—14.1	—12.6	—14.0	—12.5	—6.8	—6.5
C_{11}—O_{17}	—18.1	—16.5	—18.4	—17.0	—22.4	—20.9
$O_{10} \ldots H_{16}$	—0.4	—0.8	—14.0	—12.5	—6.8	—6.5
$O_7 \ldots O_{18}$	—0.4	—0.8	—0.4	—0.9	—6.8	—6.5
$O_{10} \ldots O_{15}$	0.3	0.3	0.3	0.3	0.8	0.6
$O_7 \ldots O_{17}$	0.3	0.3	0.3	0.3	0.8	0.6
C_3—C_4	—19.0	—18.3	—15.8	—15.3	—22.0	—20.9
C_3—C_{14}	—19.2	—18.3	—20.4	—19.6	—16.1	—16.4
C_4—O_{10}	—22.9	—21.4	—26.9	—25.5	—17.9	—17.1
C_{14}—O_{15}	—22.2	—20.5	—17.8	—16.2	—26.8	—24.7
C_4—O_5	—16.4	—15.9	—15.6	—15.1	—16.7	—16.3
C_{13}—C_{14}	—17.3	—16.9	—18.7	—18.4	—15.7	—15.6
$C_5{=}C_6$	—23.5	—22.9	—23.8	—23.1	—23.4	—22.7
C_{12}—C_{13}	—22.5	—21.8	—21.3	—20.5	—23.4	—22.6
C_1—C_6	—15.6	—15.2	—15.9	—15.4	—15.9	—15.3

TABLE VI (contd.)

	14		9		12	
	MNDO	AM1	MNDO	AM1	MNDO	AM1
C_{11}—C_{12}	—17.3	—17.0	—18.6	—18.2	—16.6	—16.1
C_{2}—C_{11}	—21.4	—20.6	—20.4	—19.6	—21.9	—21.2
C_{1}—C_{2}	—16.3	—16.0	—16.1	—15.7	—16.7	—15.7
C_{2}—C_{3}	—17.5	—17.0	—18.7	—18.3	—16.7	—16.4
$C_{1}=O_{7}$	—26.6	—24.9	—26.6	—25.0	—26.4	—25.1
O_{15}—H_{16}	—7.2	—6.9	—14.1	—12.8	—0.2	—1.0
O_{17}—H_{18}	—14.1	—12.7	—14.1	—12.7	—14.0	—12.8
C_{11}—O_{17}	—18.0	—12.5	—18.0	—16.5	—18.5	—16.6
$O_{10}\ldots H_{16}$	—6.6	—6.2	—0.2	—0.2	—14.0	—12.6
$O_{7}\ldots H_{18}$	—0.3	—0.8	—0.4	—0.8	—0.4	—0.3
$O_{10}\ldots O_{15}$	0.8	0.6	0.5	0.3	0.5	0.3
$O_{7}\ldots O_{17}$	0.3	0.3	0.3	0.3	0.3	0.3

Gross energy partitioning (AM1)

Components	*1a*	*2b*	*3*	*9*	*12*	*14*
E_1^t	—2296.5	—2296.1	—2295.1	—2296.6	—2296.3	—2295.7
E_2^t (b)	—358.1	—358.2	—360.5	—358.2	—358.1	—359.5
E_2^t (nb)	11.1	11.2	14.2	11.5	11.6	12.8
Difference						
E_1^t	0	0.4	1.0	—0.1	0.2	0.8
E_2^t (b)	0	—0.1	—2.4	—0.1	0	—1.4
E_2^t (nb)	0	0.1	3.1	0.4	0.5	1.7

6-H-2-FF (C_s), expressed as a triplet of gross energy components, reads: (1.0, —0.5, 0.2). The corresponding triplet for 9-HPO (C_{2v}) and 9-HPO (C_s) assumes the values (0.7, —0.7, 1.2). Hence, as a corollary we can say that proton tunnelling causes similar energy changes in widely different molecules. The actual numbers are, of course, somewhat different because of the difference in the size and structure of compared systems.

Formal atomic charges obtained by using approximate Mulliken prescription and molecular dipole moments are presented in Table VII. They follow the usual pattern found in MA and 6-H-2-FF and 9-HPO systems for proton tunnelling and rotation of O—H bond(s). A striking feature is the increase in the positive charge of the hydrogen atom H_{16} as its approaches the transition structure. Concomitantly, bridgehead oxygen atoms increase their electron density during this process. It should be stressed once again that keto--oxygen has always more electrons than hydroxy-oxygen implying that the 1s binding energy of the former atom is higher. This is important in discussing ESCA shifts. Other information is easily extracted by analysis of the data given in Table VII. Finally, it is interesting to notice that tautomer *1a* has a small dipole moment, but different from zero. On the other hand, the dipole moment of *2b* vanishes for symmetry reasons.

TABLE VII

Selected atomic charges and molecular dipole moments (in Debys). MNDO values are given in parentheses.

			Effective atomic charges				
Molecule	*1a*	*14*	*3*	*2a*	*8*	*9*	*10*
C_4	0.30	0.31	0.28	0.18	0.28	0.28	0.28
	(0.31)	(0.34)	(0.31)	(0.21)	(0.28)	(0.29)	(0.29)
C_3	—0.18	—0.31	—0.29	—0.23	—0.10	—0.12	—0.11
	(—0.18)	(—0.34)	(—0.31)	(—0.21)	(—0.08)	(—0.11)	(—0.10)
C_{14}	0.13	0.27	0.28	0.29	0.06	0.09	0.09
	(0.17)	(0.30)	(0.31)	(0.31)	(0.09)	(0.13)	(0.13)
O_{10}	—0.31	—0.34	—0.36	—0.25	—0.25	—0.24	—0.24
	(—0.32)	(—0.34)	(—0.36)	(—0.25)	(—0.26)	(—0.26)	(—0.26)
O_{15}	—0.25	—0.37	—0.36	—0.34	—0.25	—0.21	—0.21
	(—0.25)	(—0.37)	(—0.36)	(—0.34)	(—0.26)	(—0.22)	(—0.22)
H_{16}	0.26	0.36	0.36	0.27	0.22	0.22	0.21
	(0.23)	(0.32)	(0.32)	(0.23)	(0.20)	(0.20)	(0.20)
C_1	0.30	0.29	0.28	0.29	0.30	0.30	0.28
	(0.31)	(—0.32)	(0.31)	(0.31)	(0.31)	(0.31)	(0.29)
C_2	—0.18	—0.17	—0.29	—0.23	—0.20	—0.18	—0.11
	(—0.18)	(—0.14)	(—0.31)	(—0.21)	(—0.20)	(—0.17)	(—0.10)
C_{11}	0.13	0.12	0.28	0.18	0.15	0.12	0.09
	(0.17)	(0.15)	(0.31)	(0.21)	(0.19)	(0.16)	(0.13)
O_7	—0.31	—0.31	—0.36	—0.34	—0.31	—0.31	—0.24
	(—0.32)	(—0.25)	(—0.36)	(—0.34)	(—0.32)	(—0.32)	(—0.26)
O_{17}	—0.25	—0.25	—0.36	—0.25	—0.25	—0.26	—0.21
	(—0.25)	(—0.25)	(—0.36)	(—0.25)	(—0.25)	(—0.26)	(—0.22)
H_{18}	0.26	0.26	0.36	0.27	0.26	0.26	0.21
	(0.23)	(0.22)	(0.32)	(0.23)	(0.23)	(0.23)	(0.20)
			Molecular dipole moments				
μ	0.27	1.16	0	0	1.55	1.74	3.75
	(0.08)	(0.75)	(0)	(0)	(1.166)	(1.96)	(3.95)

CONCLUSION

Semiempirical MINDO/3, MNDO and AM1 methods give reasonable description of internal H-bonds in MA, ACAC and napthazarin tautomers. This conjecture is evidenced by comparison with the available *ab initio* results and some reliable experimental data. MINDO/3 and MNDO procedures provide qualitative information whereas the AM1 scheme is capable of yielding semiquantitative data, particularly after some empirical adjustments. It should be stressed that MINDO/3 and MNDO should not be discarded when properties of intramolecular hydrogen bonding are discussed, as some people claim.

It is found that H-bond is asymmetric in all the studied systems. Further, in napthazarin the 1,4-quinoid structure is more stable than 1,5-quinoid geometry by 9 kcal mol^{-1} according to the AM1 method. The barrier height for single proton tunnelling is 24 kcal mol^{-1} in the most stable tautomer *1a* whereas it is 9 kcal mol^{-1} lower for 1,5-quinoid geometry *2b*. Simultaneous (concerted) tunnelling of both protons in *1a* faces a barrier of 49 kcal mol^{-1}, which is roughly twice as much as in single proton transfer. Hence, two step tunnelling is energetically much more favourable. To reiterate, transfer of a single proton in *1a* forms *2b* tautomers requiring a »jump« over the barrier height of 24 kcal mol^{-1}. However, the second proton transfer forming *1a* faces a smaller barrier by 9 kcal mol^{-1}, *i. e.* that of 15 kcal mol^{-1} because of the higher energy of tautomer *2b*. The real barriers are of course lower because of the electron correlation, which is poorely described by the ordinary MO SCF procedure.

The barriers of rotation of O—H bonds and the strength of internal H-bonds are estimated and discussed in terms of micro- and gross-energy partitioning approach.

Structural features and their changes upon the proton transfer and OH rotation are considered and favourably compared with the available *ab initio* results. The same holds for the variation in atomic charges. It is found that keto- and hydroxy-oxygens have appreciably different electron densities, which necessarily lead to significant differences in ESCA chemical shifts.

Acknowledgement. — This work was partly financed by the Self-Managing Authority for Scientific Research of Croatia. Some calculations have been performed at the Organisch-chemisches Institut der Universität Heidelberg and two of us (M. E. M. and Z. B. M.) would like to thank the Alexander von Humboldt--Stiftung for financial support and Professor R. Gleiter for his hospitality.

REFERENCES

1. R. H. Blum and S. K. Carter, *Ann. Intern. Med.* **80** (1974) 249.
2. J. R. de la Vega, J. H. Busch, J. H. Schauble, K. L. Kunze, and B. E. Haggert, *J. Amer. Chem. Soc.* **104** (1982) 3295.
3. M. L. Josien, N. Fuson, J. M. Lebas, and T. M. Gregory, *J. Chem. Phys.* **21** (1953) 331.
4. D. Hadži and N. Sheppard, *Trans. Farad. Soc.* **50** (1954) 911.
5. E. Merian, *Chimica* **13** (1959) 181.
6. S. Bratan and F. Strohbusch, *J. Mol. Structure* **61** (1980) 409.
7. P. D. Cradwick and D. Hall, *Acta Cryst.* **B27** (1971) 1990.
8. H. Brockman, and A. Zeeck, *Chem. Ber.* **101** (1968) 4221.
9. H. L. Schmaud, H. Kratzin, and P. Boldt, *Justus Liebig Ann. Chem.* (1976) 1560.
10. W. I. Shiau, E. N. Duesler, I. C. Paul, D. Y. Curtin, W. H. Blann, and C. A. Fyfe, *J. Amer. Chem. Soc.* **102** (1980) 4546.
11. T. J. Zielinski, D. L. Breen, and R. Rein, *J. Amer. Chem. Soc.* **100** (1978) 6266.
12. G. Klopman, P. Andreozzi, A. J. Hopfinger, O. Kikuchi, and and M. J. S. Dewar, *J. Amer. Chem. Soc.* **100** (1978) 6286.
13. K. Ya. Burstein and A. N. Isaev, *Theoret. Chim. Acta* **64** (1984) 397.
14. M. Eckert-Maksić, P. Bishof, and Z. B. Maksić, *Croat. Chem. Acta* **58** (1985) 407; *J. Mol. Structure Theochem* **139** (1986) 1315.
15. M. Eckert-Maksić, and Lj. Maksimović, *Croat. Chem. Acta* **59** (1986) 757; *J. Mol. Structure Theochem* **153** (1987) 121.
16. E. S. Marcos, J. J. Maraver, J. L. Chiara, and A. G. Sanchez, *J. Chem. Soc. Perkin Trans. II* (1988) 2059.
17. M. J. S. Dewar and W. Thiel, *J. Amer. Chem. Soc.* **99** (1977) 4899.
18. M. J. S. Dewar, E. G. Zoebisch, E F. Healy, and J. J. P. Stewart, *J. Amer. Chem. Soc.* **107** (1985) 3902.
19. P. Schuster, *Chem. Phys. Lett.* **3** (1969) 433.
20. M. S. Gordon and R. D. Koob, *J. Amer. Chem. Soc.* **95** (1973) 5863.
21. A. D. Isaacson and K. Morokuma, *J. Amer. Chem. Soc.* **97** (1975) 4453.
22. J. E. del Bene W. L. Kochenour, *J. Amer. Chem. Soc.* **98** (1976) 2041.
23. G. Karlström, H. Wennerström, B. Jönsson, S. Forsen, J. Almlöf, and B. Roos, *J. Amer. Chem. Soc.* **97** (1975) 4188.

24. G. Karlström, B. Jönsson, B. Roos, and H. Wennerström, *J. Amer. Chem. Soc.* **98** (1976) 6851.
25. P. George, C. W. Bock, and M. Trachtman, *J. Comp. Chem.* **1** (1980) 373.
26. E. M. Fluder and J. R. de la Vega, *J. Amer. Chem. Soc.* **100** (1978) 5265.
27. A. H. Lowrey, C. George, P. D'Antonio, and J. Karle, *J. Amer. Chem. Soc.* **93** (1971) 6399; A. L. Andreassen and S. H. Bauer, *J. Mol. Struct.* **12** (1972) 381.
28. A. L. Andreassen, D. Zebelman, and S. H. Bauer, *J. Amer. Chem. Soc.* **93** (1971) 1148.
29. (a) K. Iijima, A. Ohnogi, and S. Shibata, *J. Mol. Struct.* **156** (1987) 111; (b) A. Camerman, D. Mastropolo, and N. Camerman, *J. Amer. Chem. Soc.* **105** (1983) 1584.
30. W. Egan, G. Gunnarson, T. E. Bull, and S. Forsen, *J. Amer. Chem. Soc.* **99** (1977) 4568.
31. L. M. Jackman, J. C. Trewella, and R. C. Haddon, *J. Amer. Chem. Soc.* **102** (1980) 2519.
32. Š. L. Baugheum, R. W. Duerst, W. F. Rowe, Z. Smith, and E. B. Wilson, *J. Amer. Chem. Soc.* **103** (1981) 6296.
33. R. S. Brown, A. Tse, T. Nakashima, and R. C. Haddon, *J. Amer. Chem. Soc.* **101** (1979) 3157 and the references cited therein.
34. Z. B. Maksić and K. Rupnik, *J. Mol. Struct.* **141** (1986) 309.
35. Z. B. Maksić, K. Rupnik, and M. Eckert-Maksić, *J. El. Spectry Rel. Phenom.* **16** (1979) 371.
36. (a) J. Bicerano, H. F. Schaefer III, and W. H. Miller, *J. Amer. Chem. Soc.* **105** (1983) 2550; (b) M. J. Frisch, A. C. Scheiner, H. F. Schaefer III, and J. S. Binkley, *J. Chem. Phys.* **82** (1985) 4194.
37. H. Fischer and H. Kollmar, *Theoret. Chim. Acta* **16** (1970) 163.
38. M. J. S. Dewar and D. H. Lo, *J. Amer. Chem. Soc.* **93** (1971) 7201; M. J. S. Dewar, D. H. Lo, and Z. B. Maksić, *Croat. Chem. Acta* **46** (1974) 7.
39. J. B. Moffat, *Croat. Chem. Acta* **57** (1984) 1475 and the references cited therein.
40. Z. B. Maksić, and K. Rupnik, *Croat. Chem. Acta* **56** (1983) 461.
41. Z. B. Maksić, M. Eckert-Maksić, and K. Rupnik, *Croat. Chem. Acta* **57** (1984) 1295.
42. K. Jug and Z. B. Maksić, in *Theoretical Models of Chemical Bonding*, Vol. 3., Z. B. Maksić, Ed., Springer-Verlag, Heidelberg (in print).

SAŽETAK

Semiempirijski studij intramolekularne vodikove veze u naftazarinu

Z. B. Maksić, M. Eckert-Maksić i D. Kovaček

Primijenjene su semiempirijske metode MINDO/3, MNDO i AM1 na ispitivanje strukture i svojstava tautomera naftazarina, koji imaju intramolekularnu vodikovu vezu. Postignuto je dobro slaganje s raspoloživim ab initio rezultatima i vjerodostojnim eksperimentalnim podacima.